Physics Letters B 773 (2017) 258–264

Contents lists available at ScienceDirect

Physics Letters B

www.elsevier.com/locate/physletb

Cutoff in the Lyman-α forest power spectrum: Warm IGM or warm dark matter?

Antonella Garzilli [a,*], Alexey Boyarsky [a], Oleg Ruchayskiy [b]

[a] Lorentz Institute, Leiden University, Niels Bohrweg 2, Leiden, NL-2333 CA, The Netherlands
[b] Discovery Center, Niels Bohr Institute, Blegdamsvej 17, DK-2100 Copenhagen, Denmark

ARTICLE INFO

Article history:
Received 8 July 2016
Received in revised form 19 January 2017
Accepted 14 August 2017
Available online 23 August 2017
Editor: S. Dodelson

Keywords:
Cosmology, Warm dark matter, Large scale structure of Universe
Methods, Numerical, Observational
Quasars, Absorption lines

ABSTRACT

We re-analyse high redshift and high resolution Lyman-α forest spectra considered in [1], seeking to constrain the properties of warm dark matter particles. Compared to this previous work, we consider a wider range of thermal histories of the intergalactic medium. We find that both warm and cold dark matter models can explain the cut-off observed in the flux power spectra of high-resolution observations equally well. This implies, however, very different thermal histories and underlying reionization models. We discuss how to remove this degeneracy.

1. Introduction

Dark matter is a central ingredient of the current standard cosmological model. It drives the formation of structures, and explains the masses of galaxies and galaxy clusters. If dark matter is made of particles, these yet-unseen particles should have been created in the early Universe long before the recombination epoch. If such particles were relativistic at early times, they would stream out from overdense regions, smoothing out primordial density fluctuations. The signature of such *warm dark matter* (WDM) scenario would be the suppression of the matter power spectrum at scales below their free-streaming horizon. From cosmological data at large scales (CMB and galaxy surveys) we know that such a suppression should be sought at comoving scales well below a Mpc.

The Lyman-α forest has been used for measuring the matter power spectrum at such scales [2–4]. In previous works only upper bounds had been reported on the mass of the thermal relic [5–10]. However, while in the SDSS spectra there is no cut-off in the transmitted flux power spectrum, there is a cut-off in the high resolution spectra, for example [4,11,7]. Recently [1] has observed the cut-off of the flux power spectrum at scales $k \sim 0.03$ s/km and redshifts $z = 4.2$–5.4.

However, the Lyman-α forest method measures not the distribution of dark matter itself, but only the neutral hydrogen density as a proxy for the overall matter density. The process of reionization heats the hydrogen and prevents it from clustering at small scales at the redshifts in question [12]. Therefore, the observed hydrogen distribution eventually stops to follow the DM distribution. Indeed, it was demonstrated in [1] that within ΛCDM cosmology there exists a suitable thermal history of intergalactic medium (IGM) that is consistent with the observed cutoff. This does not mean, however, that this scenario is realized in nature.

In this Letter we investigate this issue in depth. We ask whether *the cutoff in the flux power spectrum can be attributed to the suppression of small scales with warm dark matter* and what this means for the thermal history of IGM. To this end we reanalyze the data used in [1]. We use *the same* suite of hydrodynamical simulations of the IGM evolution with cold and warm dark matter models as in [1] and demonstrate that the data is described equally well by the model, where flux power spectrum suppression is mainly due to WDM.

2. Data and model

The data set is constituted by 25 high-resolution quasar spectra, in the redshift interval $4.48 \leq z_{\rm QSO} \leq 6.42$. The spectra were taken with the Keck High Resolution Echelle Spectrometer (HIRES) and the Magellan Inamory Kyocera Echelle (MIKE) spectrograph on the Magellan clay telescope. The QSO spectra are divided into four

* Corresponding author.
E-mail address: garzilli@lorentz.leidenuniv.nl (A. Garzilli).

http://dx.doi.org/10.1016/j.physletb.2017.08.022

redshift bins centered on: $z = 4.2, 4.6, 5.0, 5.4$. The resulting range of wave-numbers probed by this dataset is $k = 0.005$–0.08 s/km.

At these redshifts, the IGM is thought to be in a highly ionized state, being photo-ionized and photo-heated by early sources. Both the WDM cosmology and the IGM temperature affect the amount of flux power spectrum at small scales through three distinct physical mechanisms: (1) a suppression in the initial matter power spectrum; (2) Jeans broadening; and (3) Doppler broadening of the absorption lines [12–17]. The first mechanism is cosmological, the latter two are astrophysical. The Doppler broadening is a one dimensional smoothing effect that originates from observing the hot IGM along a line of sight. The Maxwellian distribution of velocities in the gas then leads to the broadening effect. The Jeans broadening smooths the three-dimensional underlying gas distribution relative to the dark matter.

The level of ionization is captured by *the effective optical depth*, $\tau_{\rm eff}$, that is computed from the mean flux, $\langle F \rangle$, through the relation $\langle F(z) \rangle = \exp(-\tau_{\rm eff}(z))$. Because the IGM spans a wide range of density, describing the IGM temperature may be complicated in principle. But, assuming that the IGM is heated by photo-heating, the temperature of the IGM follows a simple power-law *temperature-density relation* [18]:

$$T(\delta) = T_0(z)\left(1+\delta\right)^{\gamma(z)-1}, \tag{1}$$

where $\delta = \delta\rho_{\rm m}/\bar{\rho}_{\rm m}$ is the matter overdensity and $T_0(z)$, $\gamma(z)$ are unknown functions of redshift. The results of Ref. [1] are based on single power-law parametrizations, $T_0(z)$ and $\gamma(z)$. In this letter we let the parameters of the IGM thermal state vary independently in each redshift bin, with a total of 8 parameters describing the IGM thermal state ($T_0(z_i)$ and $\gamma(z_i)$ in 4 distinct redshift intervals).[1]

We want to point out that T_0 and γ are not varied in post-processing. The original work of [1] considered 9 simulation runs with distinct thermal histories for each cosmology considered. The different thermal histories are realized by changing the photo-heating function in the simulations. The resulting values of T_0 and γ are approximately distributed on a regular grid. In [1] the effect of Jeans smoothing is accounted by considering two additional simulation runs, where the time at which the ultraviolet background is switched on, $z_{\rm reion}$, is varied. We caution the reader that the resulting constraints on $z_{\rm reion}$ must not be intended as a measurement of the time of reionization, because this depends on the details of the implementation of the ultraviolet background. Instead, varying $z_{\rm reion}$ must be considered as a way to account for the unknown level of Jeans smoothing. Finally, as in [1], we allow the effective optical depth vary independently in each redshift bin, $\tau_{\rm eff}[z_i]$.

It should be noted that this interpolation scheme between simulations with different temperatures may also vary the amount of Jeans broadening (also known as the "filtering scale"). While the degeneracy between the WDM cosmologies and the Doppler smoothing has been extensively considered in the literature, the degeneracy between Jeans smoothing and WDM cosmology has not been considered in depth so far. In particular this has not been done for the suite of simulations in the original work [1] on which we base our analysis. We leave the study of the degeneracy between the Jeans smoothing and WDM for future work.

The results also depend on the cosmological parameters n_s, Ω_M, σ_8, H_0. However the small scale Lyman-α data by itself does not sufficiently constrain the cosmological parameters. Therefore, in the final likelihood function for these parameters we used best fit Planck values [19] with Gaussian priors (as in [1]), $\Omega_M = 0.315 \pm 0.017$, $\sigma_8 = 0.829 \pm 0.013$, $n_s = 0.9603 \pm 0.0073$.

[1] Ref. [1] also performed such a "binned analysis", see the detailed comparison below.

Table 1
Parameter estimation from Bayesian analysis. We show the 1-σ and 2-σ confidence intervals. We only show the parameters that are constrained at 1 or 2-σ level.

parameter	mean	1-σ	2-σ
H_0 [km/s/Mpc]	63	< 67	–
$m_{\rm WDM}$ [keV]	3.9	[143, 2.3]	> 2.1
$T_0(z=4.2)$ [10^3 K]	10.6	[9.4, 11.8]	[8.3, 12.9]
$T_0(z=4.6)$ [10^3 K]	9.8	[8.6, 11.1]	[7.5, 12.2]
$T_0(z=5.0)$ [10^3 K]	4.0	[2.0, 5.6]	< 6.9
$T_0(z=5.4)$ [10^3 K]	3.8	< 4.5	< 8.2
$\tau_{\rm eff}(z=4.2)$	1.12	[1.05, 1.19]	[1.00, 1.25]
$\tau_{\rm eff}(z=4.6)$	1.30	[1.21, 1.39]	[1.15, 1.47]
$\tau_{\rm eff}(z=5.0)$	1.88	[1.74, 2.00]	[1.64, 2.13]
$\tau_{\rm eff}(z=5.4)$	2.91	[2.69, 3.10]	[2.54, 3.31]
$\gamma(z=4.2)$	1.3	> 1.1	–
$\gamma(z=5.4)$	1.3	> 1.1	–

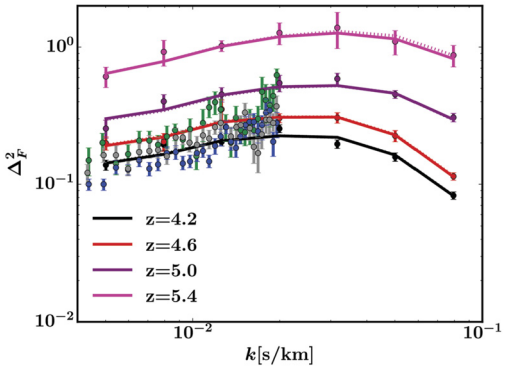

Fig. 1. Measured flux power spectrum in dimensionless units, $\Delta^2_F(k) = P_F(k) \times k/\pi$, compared with the theoretical model with the best-fitting values of the astrophysical and cosmological parameters for WDM and CDM cosmologies. The solid refer the best-fitting values for WDM cosmology. The dotted lines refer to the best-fitting case for CDM cosmology. These best-fitting models largely overlap, except at the highest redshift and on the smallest scales. The blue, gray and green points are SDSS-III/BOSS DR9 data for $z = 4.0$, $z = 4.2$ and $z = 4.4$ from [20]. (For interpretation of the references to color in this figure legend, the reader is referred to the web version of this article.)

3. Results

In Table 1 we give the result of the parameter estimation. Fig. 1 shows the theoretical flux power spectrum for the mean values of the parameters, compared with the MIKE and HIRES data used in this analysis. In order to clarify the effect of different thermal histories on our constraints, we show the effect of changing the thermal parameters (T_0 and γ) and ionization parameters ($\tau_{\rm eff}$) and the mass of the thermal relic ($1/m_{\rm wdm}$) in Fig. 2, analogous to Figs. 5 and 6 of [1].

In Fig. 3 we show the 2D confidence regions between $m_{\rm wdm}$, and $T_0 \equiv T(\delta = 0)$ (marginalizing over the other parameters). We see that at redshifts $z = 4.2$, 4.6 there is no degeneracy and an IGM temperature $T_0 \sim 10^4$ K is needed to explain the observed flux power spectrum independently of $m_{\rm wdm}$. If dark matter is "too warm" ($m_{\rm wdm} < 1.5$ keV) it produces too sharp of a cut-off in the power spectrum and is inconsistent with the data.

At the $z = 5.0$ bin the situation is different. For the masses $m_{\rm wdm} \sim 2.2$–3.3 keV even very low temperatures $T_0 \lesssim 2500$ K are consistent with the data. In this case the cutoff in the flux power spectrum is explained by WDM rather than by the temperature. The situation is analogous at $z = 5.4$. Table 1 summarizes the parameter estimation.

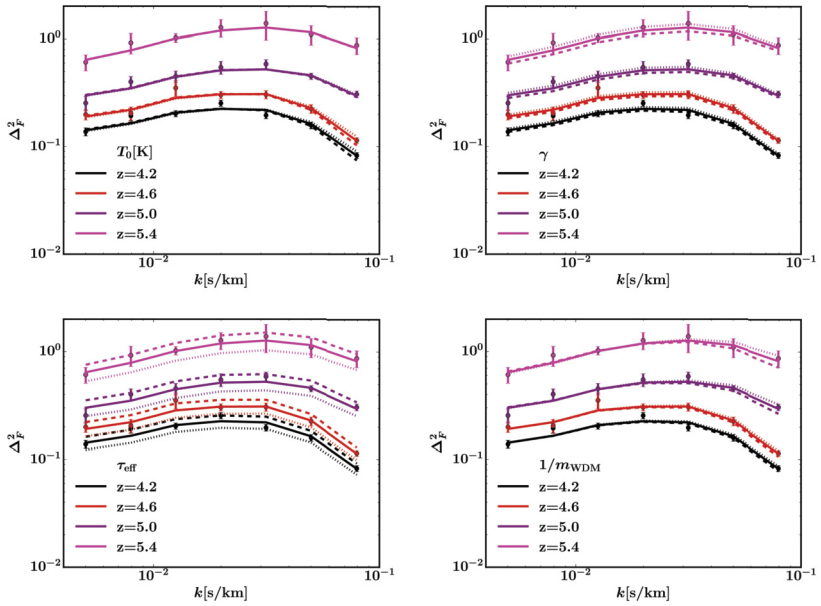

Fig. 2. Effect of the IGM parameters and $m_{\rm wdm}$ on the flux power spectrum in dimensionless units, $\Delta^2_F(k) = P_F(k) \times k/\pi$. In the top-left (top-right, bottom-left, bottom-right) panel we show the effect of varying T_0 (γ, $\tau_{\rm eff}$, $1/m_{\rm wdm}$) by $\pm 10\%$ with respect to the best-fitting values for WDM cosmology. The solid line corresponds to the best-fitting case for WDM cosmology, the dashed (dotted) line corresponds to the relevant parameter increased (decreased) by 10%. (For interpretation of the references to color in this figure legend, the reader is referred to the web version of this article.)

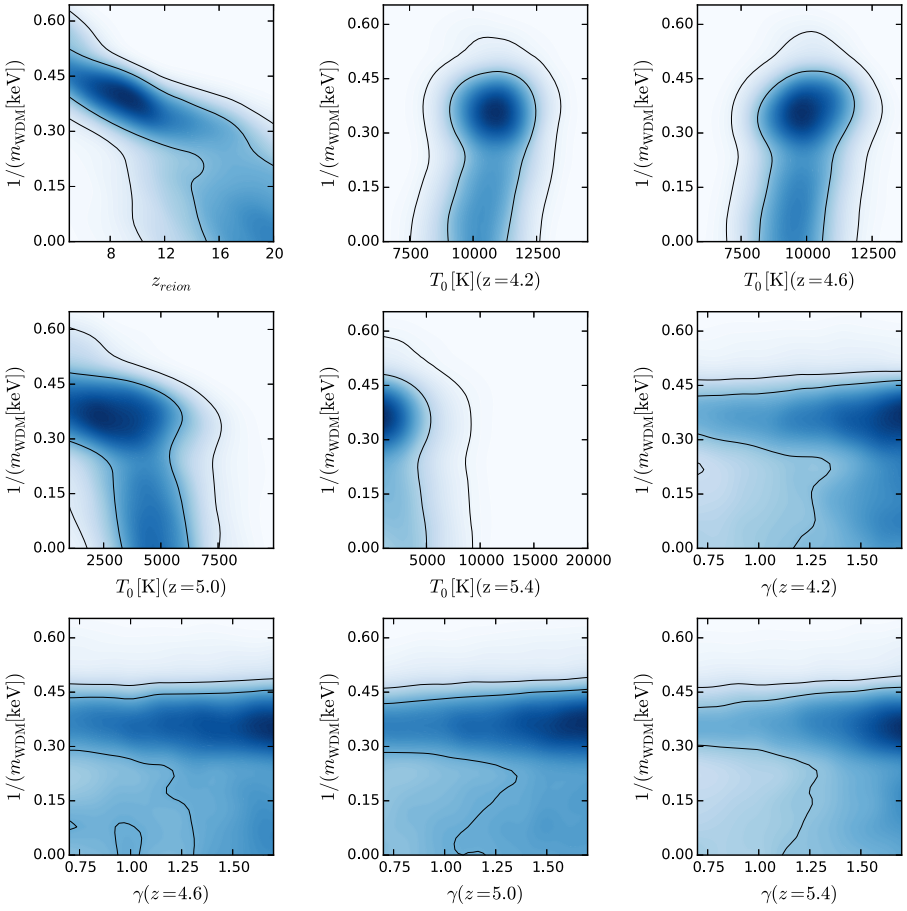

Fig. 3. Confidence regions between $m_{\rm wdm}$, and T_0 and γ at all redshift, and $z_{\rm reion}$. We show $1/m_{\rm wdm}$ instead of $m_{\rm wdm}$ for visualization purposes. $m_{\rm wdm}$ is degenerate with $z_{\rm reion}$, that is the redshift at which the ultraviolet background has been switched on in the simulations, and T_0 at the redshift $z = 5.0$. $m_{\rm wdm}$ is not degenerate with the T_0 for the other redshift intervals. There is no obvious degeneracy with γ. Regarding $m_{\rm wdm}$ and T_0, at the redshifts $z = 4.2$, 4.6 there is no degeneracy and $T_0 \sim 10^4$ K is needed to explain the observed flux power spectrum, independently of $m_{\rm wdm}$. At $z = 5.0$ even very low temperatures $T_0 \lesssim 2500$ K are consistent with the data, and the cutoff in the flux power spectrum is explained by WDM rather than by the temperature. At $z = 5.4$ the analysis prefers low values of $T_0 \sim 5 \times 10^3$ K, independently of $m_{\rm wdm}$.

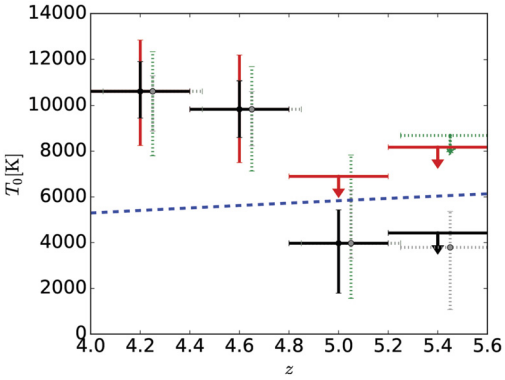

Fig. 4. The evolution of the IGM mean temperature, T_0, in redshift. Black vertical bars are 1-σ confidence limits; red vertical bars are 2-σ confidence limits. Filled dots are the parameter mean; the arrows mark the upper limits. The horizontal bars span the redshift interval of Lyman α absorbers considered for each measurement of the flux power spectrum. The solid (dotted) lines refer to the constraints on temperature for WDM (CDM) cosmology (the constraints in CDM have been shifted by $z = 0.05$ for improving the readability of the figure). At $z = 5.0$ there is a 1-σ level detection and only an upper limit at 2-σ level in WDM cosmology, instead there are both 1 and 2-σ detections for CDM cosmology. At $z = 5.4$, there are only upper limits at 1 and 2-σ levels for WDM cosmology and 1-σ detection and 2-σ upper limit for CDM cosmology. Hence, the constraints on the temperature are substantially equivalent in the two cosmologies. The blue dashed line is the asymptotic IGM mean temperature in the case of early hydrogen and first helium reionization from a stellar ionizing spectrum with slope $\alpha = 2$, being the ionizing spectrum $J_\nu \propto \nu^{-\alpha}$. (For interpretation of the references to color in this figure legend, the reader is referred to the web version of this article.)

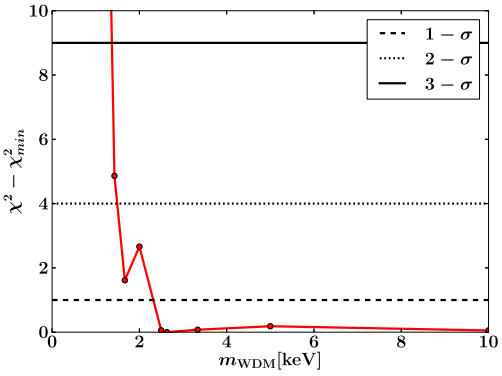

Fig. 5. The results of the frequentist analysis: the $\chi^2 - \chi^2_{min}$ versus the WDM mass, $m_{\rm WDM}$. There are two minima of the χ^2 curve, CDM and $m_{\rm wdm} = 2.7$ keV.

Another important property of Fig. 3 is that even assuming CDM cosmology, the temperature T_0 is a non-monotonic function of redshift and should be colder than ~ 8000 K at $z = 5.0$–5.4, see Fig. 4.[2]

The resulting χ^2 for the Bayesian analysis is ~ 25, for 30 degrees of freedom (49 data points − 19 free parameters). This is in agreement with the fact that the covariance matrix is uncertain and that has been multiplied by a factor that boosts the resulting error bars by 30%, with respect to the error bars computed by bootstrapping. This is done in the original analysis in order to account for presumed sample variance effect that affect other statistics like the transmitted flux PDF. The sample variance effect may affect the transmitted flux power spectrum, even if a detailed computation has not been performed.

For completeness we have also performed frequentist analysis for the same χ^2 considered in the Bayesian analysis. As shown in Fig. 5 the two analyses are in broad agreement with each other.

We would like to stress that our results depend crucially on allowing for a non-monotonic redshift dependence of $T_0(z)$. In [1] it was shown that assuming a power-law (*monotonic*) redshift dependence for $T_0(z)$ and $\gamma(z)$, one predicts higher temperatures of IGM for the same data. In this case the CDM cosmology is preferred over WDM, leading to the 2σ lower bound $m_{\rm wdm} \geq 3.3$ keV [1]. The "binned analysis" of [1] gave results similar to those, reported here. The authors of [1] however rejected these results, considering a temperature jump at $z = 5$–5.4 to be "unphysical" and arguing that the low χ^2 is a sign of overfitting.

In our opinion the present analysis implies that more data is needed to study such a scenario, as it currently does not allow to make any definitive conclusion and in particular does not allow to rule it out. Moreover, as mentioned above, the error bars in [1] were inflated by 30% and therefore we consider the reduced $\chi^2 = 25/30 \approx 0.83$ to be consistent with 1. We see that 2σ lower bound on the WDM mass relaxes down to $m_{\rm wdm} \geq 2.1$ keV (consistently with the results of binned analysis of [1]). Moreover, the non-monotonic thermal history makes the WDM with $m_{\rm wdm} = 2$–3 keV an equally good fit as CDM. The best fit values of T_0 can be inaccurate as they lie below the lowest simulation point in T_0 grid. Therefore more simulations are needed to settle this question. This is currently work in progress. In the absence of such additional studies the proposed non-monotonic thermal history cannot be ruled out based on the existing Lyman-α data.

For the interpretation of these results it is crucial to overview what is known about the thermal state of the IGM both theoretically and observationally. We argue below that the measured thermal history is in agreement with current models of galaxy formation and reionization.

4. State of the IGM at $z \sim 5$

The IGM temperature can be *determined* from the broadening of the Lyman-α absorption lines in QSO spectra [21–31,16]. Alternatively, it has been proposed to determine the IGM temperature by measuring the level of the transmitted flux [32–34,30], however there is no agreement between the two methods yet, see [35].

All the measurement of the IGM temperature in the literature assumed CDM cosmology. Because of the existing degeneracy between the IGM temperature and WDM, the assumption of the WDM cosmology could change the deduced values of the IGM temperature. Nevertheless, in the absence of such measurements, we compare our estimates for the IGM temperature with the measurements based on the CDM assumption.

The IGM temperature at $z < 5$ is constrained relatively well to be at the level $T_0 \gtrsim (8$–$10) \times 10^3$ K [25,22,27,28]. At $z = 6.0$ there is a single measurement, [29], that restricts T_0 to the range $5000 < T_0 < 10000$ K (68% CL) (see e.g. [1] for discussion). The simplest interpretation of these data (also adopted in [1]) is that the temperature is growing monotonically with redshift. Instead, given the large error bars of the measurements, and taking into account adiabating cooling one may expect a drop of temperature at $z \sim 5$ with a subsequent rise to $\sim 10^4$ K at $z \sim 4.6$ in agreement with other measurements from [25,22,27,28]. This increase in IGM temperature can be explained with an early start of HeII reionization predicted by some models of reionization by quasars, [36] (see recent discussion of such "two-component" reionization models in [37]).

In such a scenario, the temperature at $5 < z < 6$ depends on how long the first stage of reionization lasted and what the temperature of IGM was at $z \gtrsim 6$. As mentioned above, the measurement [29] at $z \sim 6$ has large uncertainties. Theoretically, $T_0(z = 6)$ depends on how early the first stage of hydrogen (and HeI) reion-

[2] The temperature values that we have estimated at high redshift could be inaccurate, because the lowest temperature in the simulation grid was 5400 K.

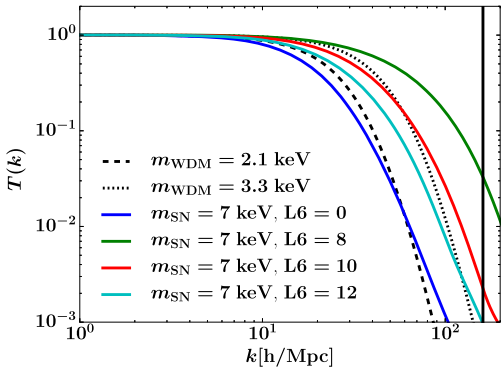

Fig. 6. Comparison between the linear transfer functions, $T(k)$, of thermal relic (WDM) and sterile neutrinos (SN). The dashed (dotted) black line is the linear transfer function for $m_{\rm WDM} = 2.1$ keV ($m_{\rm WDM} = 3.3$ keV) as computed in [10]. The colored (green, red, cyan) lines are realistic linear transfer functions for some of the sterile neutrino models with $m_{\rm SN}^{\rm NRP} = 7$ keV. The linear transfer functions with $L_6 = 10$ and 12 (red and cyan lines) are partially warmer that the lower bound of [1] (the dotted black line), but still satisfy the constraints from this letter (the dashed black line) until the maximum k-mode used in the reference numerical simulations. The linear transfer function with $L_6 = 8$ (green line) is colder than the bound of [1]. The linear transfer function with $L_6 = 0$ (blue line) violates the constraint from this letter. The solid vertical line is the maximum k-mode used in the reference simulations. (For interpretation of the references to color in this figure legend, the reader is referred to the web version of this article.)

izations has ended, and what sources drove it (cf. [38,39]). It has been speculated that hydrogen is reionized by the metal-free (Population III) stars, whose spectral hardness predicts high values of the temperature. However, the properties of Population III stars are purely speculative – we do not know how long they lasted and whether they were indeed the sources of reionization. For example, reionization could be due to a more metal rich population of stars with softer stellar spectra [40], leading to a lower values of IGM temperature at $z \sim 6$. To settle this question, an independent constraint on the ultraviolet background at high redshift would be needed, however there are no such measurements to-date. The lower limit of [29] is $T_0(z = 6) \approx 5 \times 10^3$ K or even slightly below, fully consistent with the low values at $z = 5.0$–5.4 (Table 1) reached via adiabatic cooling.

We note that an indirect argument in favour of the IGM temperatures at high redshifts being $\sim 10^4$ K, is the "missing satellite problem" – high temperature would prevent gas from collapsing into dark matter halos with a mass below $\sim 10^7 M_\odot$, thus suppressing the formation of small galaxies (see e.g. [41–44]), explaining in particular the small number of satellites of the Milky Way. However, in WDM cosmologies the matter power spectrum is suppressed at the smallest scales, thus solving the missing satellite problem even if the gas was sufficiently cooler.

Finally, we use our results to explore the constraints on sterile neutrino dark matter [45], resonantly produced in the presence of lepton asymmetry [46–48]. This is a non-thermal warm dark matter, whose primordial phase-space density distribution resembles a mixture of cold + warm dark matter components [49,50], demonstrating a shallower cut-off. In Fig. 6 we compare the linear transfer function (the square root of the ratio of the modified linear matter power spectrum to that of cold dark matter, $T(k) = \sqrt{P_{\rm WDM}(k)/P_{\rm CDM}(k)}$) of thermal relic WDM with a mass $m_{\rm wdm} = 2.1$ keV (lower bound from this work) and a $m_{\rm wdm} = 3.3$ keV [1] with those of resonantly produced sterile neutrinos with the mass 7 keV (motivated by the recent reports of an unidentified spectral line at the energy $E \sim 3.5$ keV in the stacked X-ray spectra of Andromeda galaxy, Perseus galaxy clusters, stacked galaxy clusters and the Galactic Center of the Milky Way [51–53]). We show that depending on the value of the lepton asymmetry, $L_6 \equiv 10^6(n_{\nu_e} - n_{\bar{\nu}_e})/s$ (see [50] for details) the linear power can be colder than that of thermal relics with $m_{\rm wdm} = 2.1$ keV (Fig. 6), thus being fully admissible by the data.[3] Notice that the non-resonant sterile neutrino dark matter with a 7 keV mass would be excluded at more than 3σ level by previous constraints from the SDSS [7,6].

5. Conclusion and future work

We demonstrated that the cut-off in the flux power spectrum, observed in the high resolution Lyman-α forest data may either be due to free-streaming of dark matter particles or be explained by the temperature of the intergalactic medium. Taking into account measurements at redshifts $z \sim 6$ and at $z < 5$ we see that if dark matter is *warm*, this requires non-monotonic dependence on the IGM temperature on z with the local minimum at $z \sim 5.0$–5.4. Even cold dark matter slightly prefers a non-monotonic $T_0(z)$.[4] Improving our knowledge of the IGM temperature at $z \sim 5$–6 will therefore either result in very strong Lyman-α bounds on DM free-streaming, essentially excluding its influence on observable small-scale structures, or (if temperature will be found to be well below 5000 K) would lead to the discovery of WDM.

A method that would allow to measure the IGM temperature at the redshifts of interest was presented in [16]. It is based on the following idea: for high resolution spectra it is not necessary to study average deviation from the QSO continuum per redshift bins (as it is done in lower resolution case) but it is possible to identify individual absorption lines and to measure their broadening. The thermal Doppler effect broadens the natural lorentzian line profile of the Lyman-α transition proportionally to the square root of the temperature, and one would like to use this information to determine the temperature of the IGM *directly*. However, there are other effects that contribute to the line width – the physical extent and the clustering of the underlying filaments. The method of [16] potentially allows to disentangle these effects. In view of our results it is important to attempt to apply this method to observational data. This is a method that has been tested with simulations at redshift ~ 3, and it still has to be seen if it works at redshift 5.

Acknowledgements

The authors are grateful to Matteo Viel, for sharing with them the code used in [1], and making this analysis possible. The authors thank James Bolton, Joop Schaye and Tom Theuns for useful discussions on the IGM temperature at high redshift. AG thanks Mark Lovell for sharing his knowledge about generating SN power spectra. She also thanks Bin Hu, Samuel Leach, Matteo Martinelli and Jesus Torrado for useful discussions on MCMC method. The authors thank the anonymous referee for his helpful comments, that improved the manuscript by large extent. The research was supported in part by the European Research Council under the European Union's Seventh Framework Programme (FP7/2007–2013)/ERC grant agreements 278594-GasAroundGalaxies.

[3] Our computations of the phase-space distribution functions for sterile neutrinos are based on [48] and the linear power spectrum is obtained with the modified CAMB code developed in [49]. We do not expect the most recent computations [54,55] to affect our results.

[4] As stated in [56], a model of fluctuating UVB, with spatially constant mean free path for the hydrogen-ionizing photons (similar to the one used in [1] and in this work) may not be adequate to explain the observed scatter in the optical depth at the redshifts $5.1 \leq z \leq 5.7$. Proper modeling of patchy reionization may affect the conclusions about the IGM state. We leave this for future work.

References

[1] M. Viel, G.D. Becker, J.S. Bolton, M.G. Haehnelt, Warm dark matter as a solution to the small scale crisis: new constraints from high redshift Lyman-α forest data, Phys. Rev. D 88 (2013) 043502, http://dx.doi.org/10.1103/PhysRevD.88.043502, arXiv:1306.2314.

[2] R.A.C. Croft, D.H. Weinberg, N. Katz, L. Hernquist, Recovery of the power spectrum of mass fluctuations from observations of the Lyman alpha forest, Astrophys. J. 495 (1998) 44, http://dx.doi.org/10.1086/305289, arXiv:astro-ph/9708018.

[3] P. McDonald, J. Miralda-Escude, M. Rauch, W.L.W. Sargent, T.A. Barlow, R. Cen, J.P. Ostriker, The observed probability distribution function, power spectrum, and correlation function of the transmitted flux in the Lyman-alpha forest, Astrophys. J. 543 (2000) 1–23, http://dx.doi.org/10.1086/317079, arXiv:astro-ph/9911196.

[4] R.A.C. Croft, D.H. Weinberg, M. Bolte, S. Burles, L. Hernquist, N. Katz, D. Kirkman, D. Tytler, Towards a precise measurement of matter clustering: Lyman alpha forest data at redshifts 2–4, Astrophys. J. 581 (2002) 20–52, http://dx.doi.org/10.1086/344099, arXiv:astro-ph/0012324.

[5] S.H. Hansen, J. Lesgourgues, S. Pastor, J. Silk, Constraining the window on sterile neutrinos as warm dark matter, Mon. Not. R. Astron. Soc. 333 (2002) 544–546, http://dx.doi.org/10.1046/j.1365-8711.2002.05410.x, arXiv:astro-ph/0106108.

[6] A. Boyarsky, J. Lesgourgues, O. Ruchayskiy, M. Viel, Lyman-alpha constraints on warm and on warm-plus-cold dark matter models, J. Cosmol. Astropart. Phys. 0905 (2009) 012, http://dx.doi.org/10.1088/1475-7516/2009/05/012, arXiv:0812.0010.

[7] U. Seljak, A. Makarov, P. McDonald, H. Trac, Can sterile neutrinos be the dark matter?, Phys. Rev. Lett. 97 (2006) 191303, http://dx.doi.org/10.1103/PhysRevLett.97.191303, arXiv:astro-ph/0602430.

[8] M. Viel, G.D. Becker, J.S. Bolton, M.G. Haehnelt, M. Rauch, W.L.W. Sargent, How cold is cold dark matter? Small scales constraints from the flux power spectrum of the high-redshift Lyman-alpha forest, Phys. Rev. Lett. 100 (2008) 041304, http://dx.doi.org/10.1103/PhysRevLett.100.041304, arXiv:0709.0131.

[9] M. Viel, J. Lesgourgues, M.G. Haehnelt, S. Matarrese, A. Riotto, Can sterile neutrinos be ruled out as warm dark matter candidates?, Phys. Rev. Lett. 97 (2006) 071301, http://dx.doi.org/10.1103/PhysRevLett.97.071301, arXiv:astro-ph/0605706.

[10] M. Viel, J. Lesgourgues, M.G. Haehnelt, S. Matarrese, A. Riotto, Constraining warm dark matter candidates including sterile neutrinos and light gravitinos with WMAP and the Lyman-alpha forest, Phys. Rev. D 71 (2005) 063534, http://dx.doi.org/10.1103/PhysRevD.71.063534, arXiv:astro-ph/0501562.

[11] T.S. Kim, M. Viel, M.G. Haehnelt, R.F. Carswell, S. Cristiani, The power spectrum of the flux distribution in the Lyman-alpha forest of a large sample of UVES QSO absorption spectra (LUQAS), Mon. Not. R. Astron. Soc. 347 (2004) 355, http://dx.doi.org/10.1111/j.1365-2966.2004.07221.x, arXiv:astro-ph/0308103.

[12] N.Y. Gnedin, L. Hui, Probing the universe with the Lyman alpha forest: 1. Hydrodynamics of the low density IGM, Mon. Not. R. Astron. Soc. 296 (1998) 44–55, http://dx.doi.org/10.1046/j.1365-8711.1998.01249.x.

[13] T. Theuns, J. Schaye, M.G. Haehnelt, Broadening of QSO Lyα forest absorbers, Mon. Not. R. Astron. Soc. 315 (2000) 600–610, http://dx.doi.org/10.1046/j.1365-8711.2000.03423.x.

[14] V. Desjacques, A. Nusser, Joint modeling of the probability distribution and power spectrum of the Ly-alpha forest: comparison with observations at $z = 3$, Mon. Not. R. Astron. Soc. 361 (2005) 1257–1272, http://dx.doi.org/10.1111/j.1365-2966.2005.09254.x, arXiv:astro-ph/0410618.

[15] M.S. Peeples, D.H. Weinberg, R. Dave, M.A. Fardal, N. Katz, Pressure support vs. thermal broadening in the Lyman-alpha forest I: effects of the equation of state on longitudinal structure, Mon. Not. R. Astron. Soc. 404 (2010) 1281–1294, http://dx.doi.org/10.1111/j.1365-2966.2010.16383.x, arXiv:0910.0256.

[16] A. Garzilli, T. Theuns, J. Schaye, The broadening of Lyman-α forest absorption lines, Mon. Not. R. Astron. Soc. 450 (2) (2015) 1465–1476, http://dx.doi.org/10.1093/mnras/stv394, arXiv:1502.05715.

[17] G. Kulkarni, J.F. Hennawi, J. Oñorbe, A. Rorai, V. Springel, Characterizing the pressure smoothing scale of the intergalactic medium, Astrophys. J. 812 (2015) 30, http://dx.doi.org/10.1088/0004-637X/812/1/30, arXiv:1504.00366.

[18] L. Hui, N.Y. Gnedin, Equation of state of the photoionized intergalactic medium, Mon. Not. R. Astron. Soc. 292 (1997) 27, http://dx.doi.org/10.1093/mnras/292.1.27, arXiv:astro-ph/9612232.

[19] Planck Collaboration, P.A.R. Ade, N. Aghanim, C. Armitage-Caplan, M. Arnaud, M. Ashdown, F. Atrio-Barandela, J. Aumont, C. Baccigalupi, A.J. Banday, et al., Planck 2013 results. XVI. Cosmological parameters, Astron. Astrophys. 571 (2014) A16, http://dx.doi.org/10.1051/0004-6361/201321591, arXiv:1303.5076.

[20] N. Palanque-Delabrouille, C. Yèche, A. Borde, J.-M. Le Goff, G. Rossi, M. Viel, É. Aubourg, S. Bailey, J. Bautista, M. Blomqvist, A. Bolton, J.S. Bolton, N.G. Busca, B. Carithers, R.A.C. Croft, K.S. Dawson, T. Delubac, A. Font-Ribera, S. Ho, D. Kirkby, K.-G. Lee, D. Margala, J. Miralda-Escudé, D. Muna, A.D. Myers, P. Noterdaeme, I. Pâris, P. Petitjean, M.M. Pieri, J. Rich, E. Rollinde, N.P. Ross, D.J. Schlegel, D.P. Schneider, A. Slosar, D.H. Weinberg, The one-dimensional Lyα forest power spectrum from BOSS, Astron. Astrophys. 559 (2013) A85, http://dx.doi.org/10.1051/0004-6361/201322130, arXiv:1306.5896.

[21] T. Theuns, S. Zaroubi, A wavelet analysis of QSO spectra, Mon. Not. R. Astron. Soc. 317 (2000) 989, http://dx.doi.org/10.1046/j.1365-8711.2000.03729.x, arXiv:astro-ph/0002172.

[22] P. McDonald, J. Miralda-Escude, M. Rauch, W.L.W. Sargent, T.A. Barlow, R. Cen, A measurement of the temperature-density relation in the intergalactic medium using a new Lyman-alpha absorption line fitting method, Astrophys. J. 562 (2001) 52–75, http://dx.doi.org/10.1086/323426, arXiv:astro-ph/0005553, Astrophys. J. 598 (2003) 712 (Erratum).

[23] M. Zaldarriaga, L. Hui, M. Tegmark, Constraints from the Lyman alpha forest power spectrum, Astrophys. J. 557 (2001) 519–526, http://dx.doi.org/10.1086/321652, arXiv:astro-ph/0011559.

[24] M. Viel, M.G. Haehnelt, Cosmological and astrophysical parameters from the SDSS flux power spectrum and hydrodynamical simulations of the Lyman-alpha forest, Mon. Not. R. Astron. Soc. 365 (2006) 231–244, http://dx.doi.org/10.1111/j.1365-2966.2005.09703.x, arXiv:astro-ph/0508177.

[25] J. Schaye, T. Theuns, M. Rauch, G. Efstathiou, W.L.W. Sargent, The thermal history of the intergalactic medium, Mon. Not. R. Astron. Soc. 318 (2000) 817, http://dx.doi.org/10.1046/j.1365-8711.2000.03815.x, arXiv:astro-ph/9912432.

[26] M. Ricotti, N.Y. Gnedin, J.M. Shull, The evolution of the effective equation of state of the IGM, Astrophys. J. 534 (2000) 41–56, http://dx.doi.org/10.1086/308733, arXiv:astro-ph/9906413.

[27] A. Lidz, C.A. Faucher-Giguere, A. Dall'Aglio, M. McQuinn, C. Fechner, M. Zaldarriaga, L. Hernquist, S. Dutta, A measurement of small scale structure in the $2.2 \leq z \leq 4.2$ Lyman-alpha forest, Astrophys. J. 718 (2010) 199–231, http://dx.doi.org/10.1088/0004-637X/718/1/199, arXiv:0909.5210.

[28] G.D. Becker, J.S. Bolton, M.G. Haehnelt, W.L.W. Sargent, Detection of extended He II reionization in the temperature evolution of the intergalactic medium, Mon. Not. R. Astron. Soc. 410 (2011) 1096, http://dx.doi.org/10.1111/j.1365-2966.2010.17507.x, arXiv:1008.2622.

[29] J.S. Bolton, G.D. Becker, S. Raskutti, J.S.B. Wyithe, M.G. Haehnelt, W.L.W. Sargent, Improved measurements of the intergalactic medium temperature around quasars: possible evidence for the initial stages of He II reionization at $z \sim 6$, Mon. Not. R. Astron. Soc. 419 (2012) 2880–2892, http://dx.doi.org/10.1111/j.1365-2966.2011.19929.x.

[30] A. Garzilli, J.S. Bolton, T.S. Kim, S. Leach, M. Viel, The intergalactic medium thermal history at redshift $z = 1.7$–3.2 from the Lyman alpha forest: a comparison of measurements using wavelets and the flux distribution, Mon. Not. R. Astron. Soc. 424 (2012) 1723, http://dx.doi.org/10.1111/j.1365-2966.2012.21223.x, arXiv:1202.3577.

[31] G.C. Rudie, C.C. Steidel, M. Pettini, The temperature-density relation in the intergalactic medium at Redshift $< z >= 2.4$, Astrophys. J. 757 (2012) L30, http://dx.doi.org/10.1088/2041-8205/757/2/L30, arXiv:1209.0005.

[32] J.S. Bolton, M. Viel, T.S. Kim, M.G. Haehnelt, R.F. Carswell, Possible evidence for an inverted temperature-density relation in the intergalactic medium from the flux distribution of the Lyman-alpha forest, Mon. Not. R. Astron. Soc. 386 (2008) 1131–1144, http://dx.doi.org/10.1111/j.1365-2966.2008.13114.x, arXiv:0711.2064.

[33] M. Viel, J.S. Bolton, M.G. Haehnelt, Cosmological and astrophysical constraints from the Lyman-alpha forest flux probability distribution function, Mon. Not. R. Astron. Soc. 399 (2009) L39–L43, http://dx.doi.org/10.1111/j.1745-3933.2009.00720.x, arXiv:0907.2927.

[34] F. Calura, E. Tescari, V. D'Odorico, M. Viel, S. Cristiani, T.S. Kim, J.S. Bolton, The Lyman alpha forest flux probability distribution at $z > 3$, Mon. Not. R. Astron. Soc. 422 (2012) 3019, http://dx.doi.org/10.1111/j.1365-2966.2012.20811.x, arXiv:1201.5121.

[35] E. Rollinde, T. Theuns, J. Schaye, I. Pâris, P. Petitjean, Sample variance and Lyman α forest transmission statistics, Mon. Not. R. Astron. Soc. 428 (2013) 540–550, http://dx.doi.org/10.1093/mnras/sts057.

[36] M. McQuinn, A. Lidz, M. Zaldarriaga, L. Hernquist, P.F. Hopkins, S. Dutta, C.-A. Faucher-Giguère, He II reionization and its effect on the intergalactic medium, Astrophys. J. 694 (2009) 842–866, http://dx.doi.org/10.1088/0004-637X/694/2/842.

[37] P. Madau, F. Haardt, Cosmic reionization after Planck: could quasars do it all?, arXiv:1507.07678.

[38] F. Haardt, P. Madau, Radiative transfer in a clumpy universe. II. The ultraviolet extragalactic background, Astrophys. J. 461 (1996) 20, http://dx.doi.org/10.1086/177035.

[39] L. Hui, Z. Haiman, The thermal memory of reionization history, Astrophys. J. 596 (2003) 9–18, http://dx.doi.org/10.1086/377229.

[40] B. Ciardi, A. Ferrara, The first cosmic structures and their effects, Space Sci. Rev. 116 (2005) 625–705, http://dx.doi.org/10.1007/s11214-005-3592-0.

[41] A.J. Benson, C.G. Lacey, C.M. Baugh, S. Cole, C.S. Frenk, The effects of photoionization on galaxy formation. 1. Model and results at $z = 0$, Mon. Not. R. Astron. Soc. 333 (2002) 156, http://dx.doi.org/10.1046/j.1365-8711.2002.05387.x, arXiv:astro-ph/0108217.

[42] A.J. Benson, C.S. Frenk, C.G. Lacey, C.M. Baugh, S. Cole, The effects of photoionization on galaxy formation. 2. Satellites in the local group, Mon. Not. R. Astron. Soc. 333 (2002) 177, http://dx.doi.org/10.1046/j.1365-8711.2002.05388.x, arXiv:astro-ph/0108218.

[43] A.V. Maccio', X. Kang, F. Fontanot, R.S. Somerville, S.E. Koposov, et al., On the origin and properties of Ultrafaint Milky Way Satellites in a LCDM Universe, Mon. Not. R. Astron. Soc. 402 (2009) 1995–2008, http://dx.doi.org/10.1111/j.1365-2966.2009.16031.x.

[44] T. Sawala, C.S. Frenk, A. Fattahi, J.F. Navarro, R.G. Bower, R.A. Crain, C. Dalla Vecchia, M. Furlong, A. Jenkins, I.G. McCarthy, Y. Qu, M. Schaller, J. Schaye, T. Theuns, Bent by baryons: the low mass galaxy-halo relation, ArXiv e-prints.

[45] S. Dodelson, L.M. Widrow, Sterile-neutrinos as dark matter, Phys. Rev. Lett. 72 (1994) 17–20, http://dx.doi.org/10.1103/PhysRevLett.72.17, arXiv:hep-ph/9303287.

[46] X.-D. Shi, G.M. Fuller, A new dark matter candidate: nonthermal sterile neutrinos, Phys. Rev. Lett. 82 (1999) 2832–2835, http://dx.doi.org/10.1103/PhysRevLett.82.2832, arXiv:astro-ph/9810076.

[47] K. Abazajian, G.M. Fuller, M. Patel, Sterile neutrino hot, warm, and cold dark matter, Phys. Rev. D 64 (2001) 023501, http://dx.doi.org/10.1103/PhysRevD.64.023501.

[48] M. Laine, M. Shaposhnikov, Sterile neutrino dark matter as a consequence of nuMSM-induced lepton asymmetry, J. Cosmol. Astropart. Phys. 0806 (2008) 031, http://dx.doi.org/10.1088/1475-7516/2008/06/031, arXiv:0804.4543.

[49] A. Boyarsky, J. Lesgourgues, O. Ruchayskiy, M. Viel, Realistic sterile neutrino dark matter with keV mass does not contradict cosmological bounds, Phys. Rev. Lett. 102 (2009) 201304, http://dx.doi.org/10.1103/PhysRevLett.102.201304, arXiv:0812.3256.

[50] A. Boyarsky, O. Ruchayskiy, M. Shaposhnikov, The role of sterile neutrinos in cosmology and astrophysics, Annu. Rev. Nucl. Part. Sci. 59 (2009) 191–214, http://dx.doi.org/10.1146/annurev.nucl.010909.083654, arXiv:0901.0011.

[51] E. Bulbul, M. Markevitch, A. Foster, R.K. Smith, M. Loewenstein, S.W. Randall, Detection of an unidentified emission line in the stacked X-ray spectrum of galaxy clusters, Astrophys. J. 789 (2014) 13, http://dx.doi.org/10.1088/0004-637X/789/1/13, arXiv:1402.2301.

[52] A. Boyarsky, O. Ruchayskiy, D. Iakubovskyi, J. Franse, Unidentified line in X-ray spectra of the Andromeda galaxy and Perseus galaxy cluster, Phys. Rev. Lett. 113 (2014) 251301, http://dx.doi.org/10.1103/PhysRevLett.113.251301, arXiv:1402.4119.

[53] A. Boyarsky, J. Franse, D. Iakubovskyi, O. Ruchayskiy, Checking the dark matter origin of 3.53 keV line with the Milky Way center, Phys. Rev. Lett. 115 (16) (2015) 161301, http://dx.doi.org/10.1103/PhysRevLett.115.161301, arXiv:1408.2503.

[54] J. Ghiglieri, M. Laine, Improved determination of sterile neutrino dark matter spectrum, arXiv:1506.06752.

[55] T. Venumadhav, F.-Y. Cyr-Racine, K.N. Abazajian, C.M. Hirata, Sterile neutrino dark matter: a tale of weak interactions in the strong coupling epoch, arXiv:1507.06655.

[56] G.D. Becker, J.S. Bolton, P. Madau, M. Pettini, E.V. Ryan-Weber, B.P. Venemans, Evidence of patchy hydrogen reionization from an extreme Lyα trough below redshift six, Mon. Not. R. Astron. Soc. 447 (2015) 3402, http://dx.doi.org/10.1093/mnras/stu2646, arXiv:1407.4850.